

Crack blunting, crack bridging and resistance-curve fracture mechanics in dentin: effect of hydration

J.J. Kruzic^a, R.K. Nalla^a, J.H. Kinney^b, R.O. Ritchie^{a,*}

^aDepartment of Materials Science and Engineering and Materials Sciences Division, Lawrence Berkeley National Laboratory, University of California, MC #1760, Berkeley, CA 94720, USA

^bLawrence Livermore National Laboratory, Livermore, CA 94550, USA

Received 18 June 2003; accepted 21 June 2003

Abstract

Few studies have focused on a description of the fracture toughness properties of dentin in terms of resistance-curve (R-curve) behavior, i.e., fracture resistance increasing with crack extension, particularly in light of the relevant toughening mechanisms involved. Accordingly, in the present study, fracture mechanics based experiments were conducted on elephant dentin in order to determine such R-curves, to identify the salient toughening mechanisms and to discern how hydration may affect their potency. Crack bridging by uncracked ligaments, observed directly by microscopy and X-ray tomography, was identified as a major toughening mechanism, with further experimental evidence provided by compliance-based experiments. In addition, with hydration, dentin was observed to display significant crack blunting leading to a higher overall fracture resistance than in the dehydrated material. The results of this work are deemed to be of importance from the perspective of modeling the fracture behavior of dentin and in predicting its failure in vivo.

© 2003 Elsevier Ltd. All rights reserved.

Keywords: Dentin; Fracture; Hydration; Toughening; Uncracked-ligament bridging; Crack blunting

1. Introduction

Dentin is a calcified tissue that makes up the bulk of the teeth; it is physically located between the exterior enamel and the interior pulp chamber. Human dentin is a hydrated composite composed of nanocrystalline carbonated apatite mineral (~45% by volume), type-I collagen fibrils (~30% by volume) and fluid (~25% by volume). The mineral is distributed in the form of 5 nm thick crystallites in a scaffold created by the collagen fibrils (50–100 nm diameter). The inorganic mineral is believed to provide the strength and the organic collagen the toughness [1]. The distinctive feature of the microstructure is the distribution of cylindrical tubules (1–2 μm diameter) that run from the dentin-enamel junction to the soft, interior pulp. These tubules are surrounded by a collar of highly mineralized peritubular dentin (~1 μm thick) and are embedded within a matrix

of mineralized collagen, called intertubular dentin [2]. The mineralized collagen fibrils form a planar felt-like structure oriented perpendicular to the tubules [3]. The fluid is located mainly in these tubules (75%), with the rest being distributed within the intertubular matrix [4].

A mechanistic understanding of the mechanical properties of dentin is important from the perspective of developing a framework for failure prediction in human teeth, particularly in light of the effect of microstructural modifications from caries, sclerosis, aging and restorative processes. In this context, it has been recognized that such properties, especially resistance to fracture, are strongly influenced by the degree of hydration [5]. Indeed, from a clinical perspective, the higher incidence of fracture in endodontically repaired teeth (with pulp replaced) has been attributed to decreased hydration, although this is still a controversial issue [6–8]. Despite the obvious importance of the effect of hydration on fracture behavior, there are only a handful of studies to date that attempt to address this issue. Early studies [9,10] used a “work of fracture” (defined as the work per unit area to generate new crack

*Corresponding author. Tel.: +1-541-486-5798; fax: +1-510-486-4881.

E-mail address: roritchie@lbl.gov (R.O. Ritchie).

surface) to quantify the toughness of human dentin and enamel in an aqueous environment; unfortunately, as this parameter is both geometry- and sample-size dependent, the results cannot be compared quantitatively with other measurements. A subsequent study [11] utilized a fracture mechanics-based approach and reported a fracture toughness¹ value of $K_c = 3.08 \text{ MPa}\sqrt{\text{m}}$ for an orientation parallel to the tubules in hydrated human dentin; this toughness was found to remain constant over the temperature range 0–60°C. Later work [12] specifically examined the effect of hydration in human dentin and revealed an increase in the strain to failure on hydration, although the failure stresses were unaffected.

A more recent study (using pre-cracked samples) in hydrated human dentin reported a *worst-case* fracture toughness value of $K_c = 1.8 \text{ MPa}\sqrt{\text{m}}$ for the orientation perpendicular to the tubules [13].² Using similar techniques, K_c values of 1.6–2.6 $\text{MPa}\sqrt{\text{m}}$ (depending upon orientation) were reported for hydrated elephant dentin [14]. This latter study identified the salient toughening mechanisms in dentin, most notably crack bridging by uncracked ligaments and collagen fibers. Finally, Kahler et al. [7] noted a significant effect of hydration on the toughness of bovine dentin (G_c values were reduced from 554 ± 27.7 to $113 \pm 17.8 \text{ J/m}^2$ on dehydration), and suggested several toughening mechanisms, including crack bridging, to explain such behavior.

While the use of K_c and G_c as single-value measures of the toughness are appropriate for many ductile and brittle materials, in some cases the fracture resistance, defined by the value of K or G , actually increases with crack extension, requiring a resistance-curve (R-curve) fracture mechanics approach [15,16]. In particular, R-curves are necessary to describe the fracture resistance of materials toughened by crack-tip shielding [17–19], i.e., mechanisms such as crack bridging, constrained microcracking, or in situ phase transformations which develop in the crack wake as the crack extends. In such instances, crack extension commences at a *crack-initiation toughness*, K_0 or G_0 , and with further crack extension requires a higher driving force until typically a “plateau” or steady-state toughness is reached. The

corresponding slope of the R-curve can be considered as measure of the *crack-growth toughness*.

Given that several of these toughening mechanisms, specifically bridging and microcracking, have been observed in other mineralized tissues [20–22], R-curve analysis can be considered to be a more appropriate means to characterize the fracture toughness of dentin. In fact, some load-extension results have been reported for bovine dentin which do suggest such resistance-curve behavior [7,23], although a comprehensive investigation has not been performed. Accordingly, the present work seeks to address this issue through a systematic study of the in vitro R-curve behavior of hydrated and dehydrated dentin, with emphasis on identifying the salient toughening mechanisms involved.

2. Materials and methods

2.1. Materials

Fractured shards of elephant tusk from an adult male elephant (*Loxodonta africana*) were used in this study; the bulk of this material, which is commonly referred to as ivory, is composed of dentin. Akin to human dentin, the characteristic feature of elephant tusk dentin is the tubules that sit in a matrix formed by the mineralized collagen fibers. Although microstructurally very similar to human dentin, there are some differences: the tubules are more elliptical in shape [24] and the peritubular cuff is comparatively very small. However, given the larger size scales involved, elephant dentin avoids the sample size restrictions of human dentin.

To measure the toughness, compact-tension, $C(T)$, specimens ($N = 16$), were machined from the shards with specimen thicknesses of $B \sim 1.2\text{--}3.3 \text{ mm}$, widths of $W \sim 13\text{--}18.3 \text{ mm}$ and initial notch lengths of $a_0 \sim 3.1\text{--}5.5 \text{ mm}$. The samples were orientated such that the nominal crack growth direction was perpendicular to the long axis of the tubules and the crack plane was in the plane of the tubules. These specimens were then polished to a 1200 grit finish, followed by polishing steps using a 1 μm alumina suspension and finally a 0.05 μm alumina suspension. The notch was introduced with a low speed diamond saw before final razor-micronotching to a root radius of $\sim 15 \mu\text{m}$; the latter was achieved by repeatedly sliding a razor blade over the saw-cut notch while irrigating with a 1 μm diamond slurry. All specimens were kept hydrated throughout preparation and prior to testing.

In order to obtain lower bound, geometry-independent toughness values, a condition of plane strain is required. According to ASTM Standard E-399, this is achieved when the sample thickness is greater than $2.5(K_c/\sigma_y)^2$, i.e., the thickness is significantly larger than the plastic or damage zone size of $r_y \sim 1/2\pi(K_c/\sigma_y)^2$,

¹The fracture toughness, K_c , is the critical stress intensity for unstable fracture at a pre-existing crack, i.e., when $K = Q\sigma_{\text{app}}(\pi a)^{1/2} = K_c$, where σ_{app} is the applied stress, a is the crack length, and Q is a function (of order unity) of crack size and geometry. Alternatively, the toughness can be expressed as a critical value of the strain energy release rate, G_c , defined as the change in potential energy per unit increase in crack area, i.e., when $G_c = K_c^2/E'$, where E' is the appropriate elastic modulus.

²These authors demonstrated a marked effect of notch acuity on the toughness values, thereby indicating that earlier measurements of the fracture toughness of dentin, which used notched rather than pre-cracked samples (e.g., [11]), gave unrealistically high values.

where σ_y is the yield strength or more appropriately the stress to cause inelastic deformation. For elephant dentin, where σ_y was measured to be ~ 75 MPa, this requires samples thicknesses greater than ~ 0.4 – 5 mm to yield plane-strain toughness values. However, as this criterion is generally quite conservative and the damage zone was well contained within the specimen boundaries, it is believed that in the current tests, conditions close to plane strain were maintained.

2.2. R-curve testing—hydrated vs. dehydrated dentin

R-curves were measured to evaluate the resistance to fracture in terms of the stress intensity, K , as a function of crack extension, Δa . The $C(T)$ specimens were loaded in displacement control using standard servo-hydraulic testing machines until the onset of cracking, which was determined by an initial drop in load. At this point, the sample was unloaded by 10–20% of the peak load to record the sample compliance at the new crack length. This process was repeated at regular intervals until the end of the test, at which point the compliance and loading data were analyzed to determine fracture resistance, K_R , as a function of Δa . Crack lengths, a , were calculated from the compliance data obtained during the test using standard $C(T)$ load-line compliance calibrations [25]:

$$a/W = 1.0002 - 4.0632U + 11.242U^2 - 106.04U^3 + 464.33U^4 - 650.68U^5, \quad (1)$$

where U is a fitting function written as

$$U = \frac{1}{(FC)^{1/2} + 1}, \quad (2)$$

where C is the sample compliance and F is a calibration constant, taken to be that which gives the best agreement between the initial compliance and optically measured crack length at the beginning of the test. Due to crack bridging, errors can occur in the compliance-crack length measurements. Consequently, re-calibration to the actual crack length was performed periodically using optical microscopy to validate the measured crack lengths; any discrepancies between the compliance and optically measured crack lengths were then corrected by assuming that the error accumulated linearly with crack extension.

Hydrated specimens ($N = 5$) were prepared by soaking in Hanks' balanced salt solution (HBSS) for at least 40 h prior to actual testing. The tests were conducted in ambient air (25°C, 20–40% relative humidity) with the specimens being continuously irrigated with HBSS while testing. The sample load-line compliance was measured using a capacitance displacement gauge attached to the gripping fixture. For the dehydrated specimens ($N = 6$), the specimens were placed in a vacuum chamber and pumped to ~ 0.1 Pa; this caused spontaneous cracking

from the notch, presumably due to the presence of residual machining stresses there. The specimens were then temporarily removed from the chamber to measure the initial crack length. Typically, weight loss due to such dehydration was ~ 5.45 (± 0.65)% of the initial weight. R-curve testing was conducted in vacuo after pumping the vacuum chamber overnight (~ 0.1 Pa) to eliminate any traces of moisture picked up during crack length measurement. The load-line compliance, in this case, was determined using a linear variable-displacement transducer (LVDT) in the load frame. Additionally, similar experiments ($N = 2$ hydrated, $N = 1$ dehydrated) were conducted using an in situ loading fixture in an optical microscope for hydrated specimens, and in a scanning electron microscope for dehydrated specimens; such experiments enabled direct observation of the fracture mechanisms involved. In addition, two ($N = 2$) “dehydrated-rehydrated” experiments were conducted wherein an R-curve test was initiated with a dehydrated sample and interrupted after some crack extension; the sample was then exposed to air, and rehydrated with HBSS in situ on the loading frame, after which the test was immediately resumed with continuous irrigation of the specimen. These experiments were conducted for the purpose of understanding the change in fracture mechanisms with hydration. Post-test observations of fracture surfaces and crack paths were obtained using optical microscopy and scanning electron microscopy (SEM).

2.3. X-ray computed tomography

In order to examine the behavior of cracks in the interior of the sample, as opposed to just the surface, synchrotron radiation computed tomography was performed on one hydrated and one dehydrated specimen at the Stanford Synchrotron Radiation Laboratory, Menlo Park, CA, to investigate bridging throughout the thickness of the specimen. Three-dimensional computed tomography was performed with monochromatic 25 keV X-rays, and the tomography data were reconstructed into three-dimensional images by the Fourier-filtered back-projection algorithm. Full details of this technique are described elsewhere [26].

2.4. Theoretical compliance calculations

In order to establish that toughening by crack bridging does occur in elephant dentin, experiments were conducted to verify that the observed bridges indeed sustain some of the applied load. Specifically, load-line compliance measurements were made before and after R-curve testing. Based on the initial compliance measurement for the notched sample (i.e., with no bridging), predictions of the theoretical bridge-free compliance can be made for any crack length using

the compliance calibrations of Saxena and Hudak [25]:

$$C = \frac{1}{F} \left(\frac{1 + a/W}{1 - a/W} \right)^2 (2.1630 + 12.219a/W - 20.065(a/W)^2 - 0.9925(a/W)^3 + 20.609(a/W)^4 - 9.9314(a/W)^5), \quad (3)$$

where all variables have been previously defined and F is determined at the beginning of the experiment for the bridge-free configuration. The theoretical compliance may be calculated using Eq. (3), and then compared to the measured compliance. If these two compliance values are equal, there is no load sustained by the bridges and the crack faces are traction-free; however, a smaller measured compliance indicates that part of the applied load is sustained by the bridges in the crack wake. This is due to the fact that load-sustaining bridges resist crack opening, resulting in a stiffer, less compliant, sample.

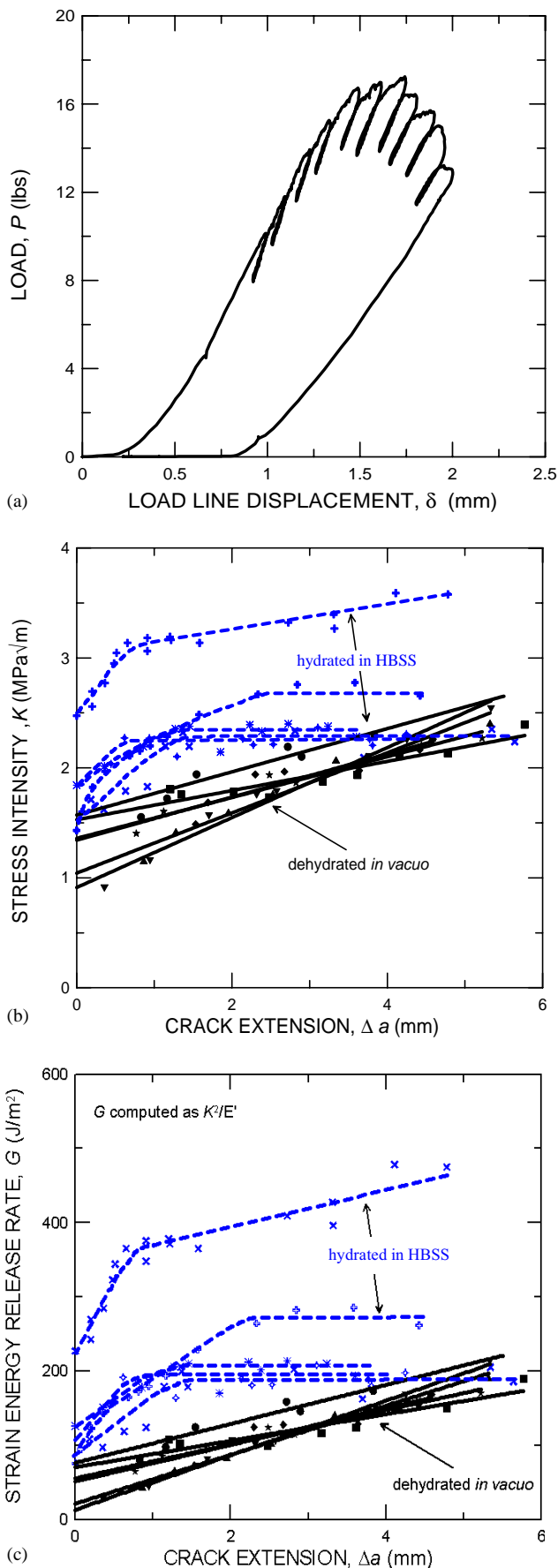
3. Results

3.1. Resistance-curve behavior

Load-displacement data (e.g., Fig. 1a) were analyzed to evaluate the resistance to fracture in terms of the stress intensity, K , as a function of crack extension, Δa ; the resulting R-curves for hydrated and dehydrated dentin are shown in Fig. 1b. In both conditions, cracks can be seen to grow subcritically for between 4 and 6 mm prior to the conclusion of the test. The dehydrated specimens, however, showed a lower crack-initiation toughness, $K_0 = 1.18 \pm 0.20 \text{ MPa}\sqrt{\text{m}}$, as compared to $1.88 \pm 0.40 \text{ MPa}\sqrt{\text{m}}$ for the hydrated specimens; this difference was statistically significant ($p = 0.004$, ANOVA). The slope of the R-curves for dehydrated dentin can be seen to be monotonically rising and distinctly shallower ($0.26 \pm 0.05 \text{ MPa}\sqrt{\text{m}/\text{mm}}$) than for hydrated dentin, which displayed an initially steep slope ($0.54 \pm 0.16 \text{ MPa}\sqrt{\text{m}/\text{mm}}$) followed by a statistically significant ($p = 0.00015$, ANOVA) “plateau” region (of slope $0.06 \pm 0.04 \text{ MPa}\sqrt{\text{m}/\text{mm}}$), where the toughness remained essentially constant with crack extension. A comparison of the initial slopes of these R-curves for hydrated vs. dehydrated dentin revealed significant differences ($p = 0.002$, ANOVA).

This difference in the fracture toughness of hydrated vs. dehydrated dentin is perhaps better expressed when

Fig. 1. (a) Typical load/load-line displacement curve for stable crack extension in dehydrated dentin, (b) $K_R(\Delta a)$ resistance-curves for hydrated and dehydrated dentin. Note the significantly higher initial increase in toughness with crack extension for hydrated dentin. (c) Data re-plotted as $G_R(\Delta a)$ R-curve for both hydrated and dehydrated dentin.



the R-curves are represented in terms of the strain-energy release rate, G (Fig. 1c). Since the process of dehydration increases the elastic modulus of dentin by some 17%, expressed in terms of G , hydration can be seen to lead to an $\sim 185\%$ increase in the steady-state toughness of dentin.

In corresponding “dehydrated-rehydrated” tests, where the degree of hydration was changed during the test, rehydration was observed to markedly elevate the maximum load sustained by the specimen (Fig. 2a); the corresponding increase in the R-curve toughness can be

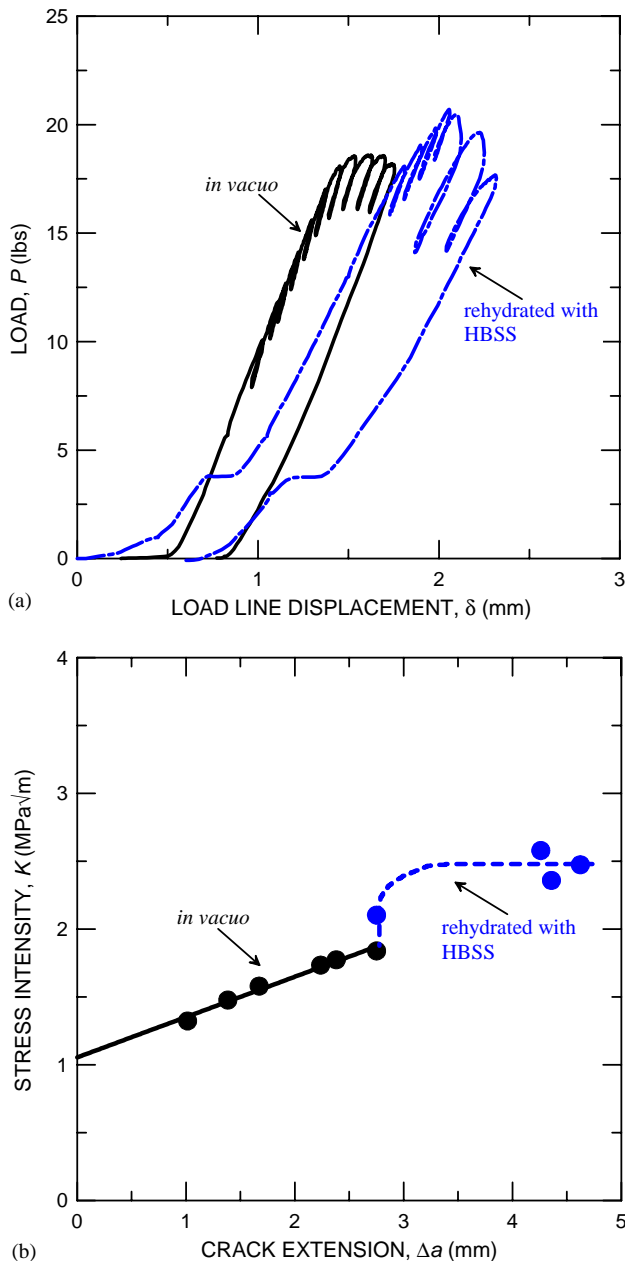


Fig. 2. Results of the “dehydrated-rehydrated” test showing (a) the load/load-line displacement curve, and (b) the resulting $K_R(\Delta a)$ resistance-curve. Note the instantaneous increase in measured toughness on hydration.

seen in Fig. 2b. After rehydration, the specimens were observed to behave very much like hydrated dentin, with an initially rising R-curve that levels out.

3.2. Crack growth observations

The R-curve tests also allowed for stable crack extension in dentin, making it possible to examine the relevant toughening mechanisms and the influence of hydration on the fracture behavior. Fig. 3a shows a typical crack emanating from the notch in hydrated dentin. The discontinuous nature of the crack path indicates extensive formation of uncracked ligaments behind the crack tip and consequent out-of-plane deflection of the crack. Such ligaments, some of them several hundred micrometers in size, act to bridge the crack, and have been previously identified as a prime toughening mechanism in elephant dentin [14]. Similar observations have been reported recently for bovine dentin [7]. Furthermore, the X-ray tomography experiments described in Section 2.3 provided strong support for the existence of such uncracked ligaments throughout the bulk of the specimen. Fig. 3b shows reconstructed through-thickness slices at different crack lengths for the hydrated specimen from Fig. 3a; again, there is clear evidence of uncracked ligaments spanning the crack.

A typical crack path in dehydrated dentin is shown in Fig. 4a. In contrast to hydrated dentin, the crack path was comparatively free of tortuosity. There appears to be minimal evidence of uncracked-ligament formation on the surface, consistent with observations by Kahler et al. [7]. However, the reconstructed tomographic images (Fig. 4b) show definite evidence of substantial ligaments in the crack wake towards the middle of the specimen. In addition, it is evident that the crack-opening displacements were significantly smaller than in hydrated dentin. In situ observations in the SEM revealed crack extension to occur by tubules close to the crack tip “opening up” and forming microracks, which then linked back to the main crack. Fig. 4c shows a series of scanning electron micrographs taken during an in situ test illustrating this. As is evident from the higher magnification inset, the size of these *near-tip* uncracked ligaments in dehydrated dentin was much smaller (typically $\leq 10\text{--}20\ \mu\text{m}$) than both the subsurface ligaments observed by tomography (Fig. 4b) and the ligaments in the hydrated samples (Fig. 3).

As noted above, a major difference between hydrated vs. dehydrated dentin was the larger crack-opening displacements observed with hydration. Such larger crack openings persisted even after unloading and were an indication that permanent plastic deformation, specifically crack blunting, had occurred at the crack tip. This is evident from the optical micrographs (Figs. 3a and 4a) and the tomographic reconstructions (Figs.

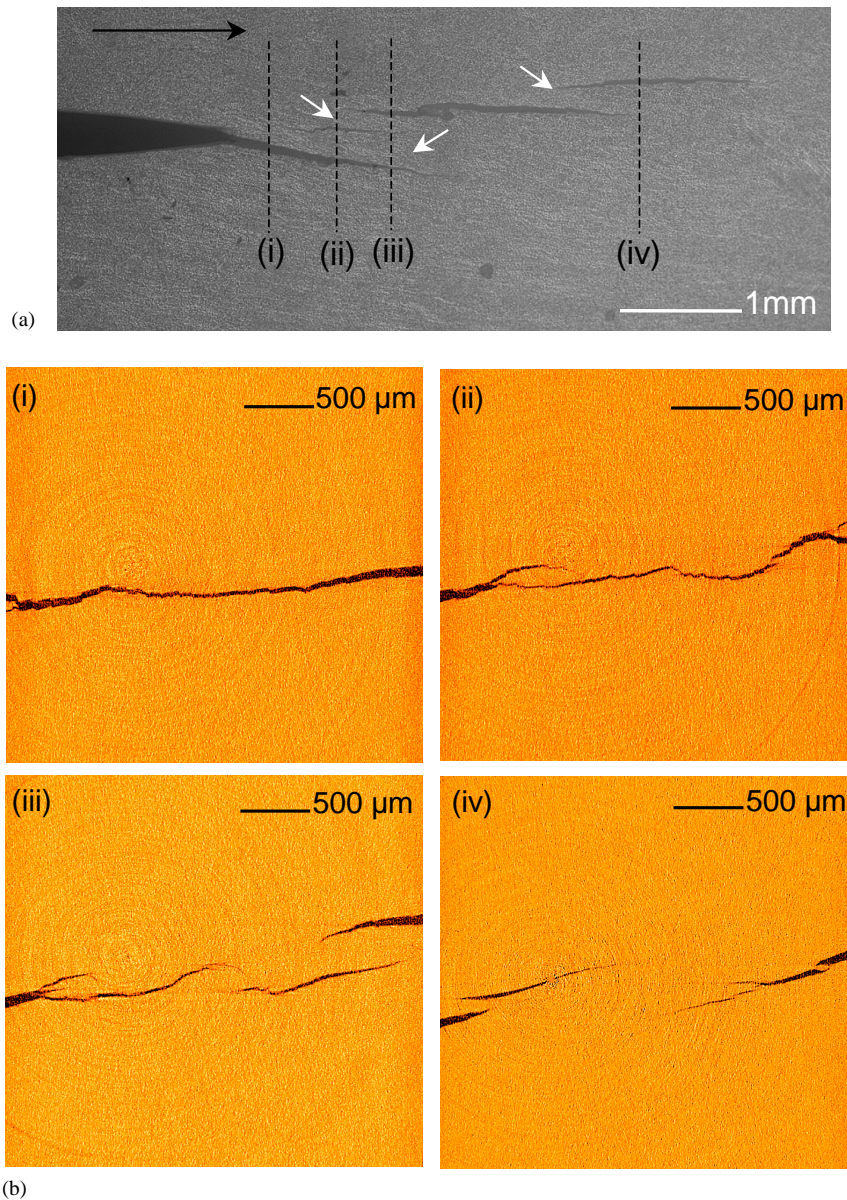


Fig. 3. (a) Optical micrograph showing the formation of uncracked-ligament bridges (indicated by white arrows) in hydrated dentin. The black arrow indicates the direction of nominal crack growth. (b) Reconstructed computed X-ray tomography slices (at positions shown by the dotted lines in (a)) showing the three-dimensional *through-thickness* nature of such ligament formation.

3b and 4b), which were all taken at zero applied load. Furthermore, on holding at a constant load-line displacement, as was performed during the in situ hydrated experiments, crack blunting continued to occur with time while the load on the sample dropped, suggesting some form of viscoplastic behavior at the crack tip. Fig. 5 shows a time-elapsing sequence of optical micrographs illustrating this phenomenon, where prior to each photo the sample was unloaded to illustrate the permanent deformation that had occurred. Although there is some crack growth initially over the first hour, these micrographs provide clear evidence of a time-dependent crack-blunting phenomenon. Additionally, in situ observations of the initial time-dependent

crack extension revealed that fluid was “squeezed out” from tubules in the blunted region surrounding the crack tip prior to the next extension of the crack. Such observations are in apparent contrast with those of Kahler et al. [7], where they report fluid ingress at the crack tip and its egress in the crack wake during subcritical cracking in hydrated dentin; no such behavior was observed in the current tests.

3.3. Theoretical compliance calculations

To provide experimental verification of the occurrence of crack bridging, measurements of the elastic compliance (inverse stiffness) of cracked specimens were

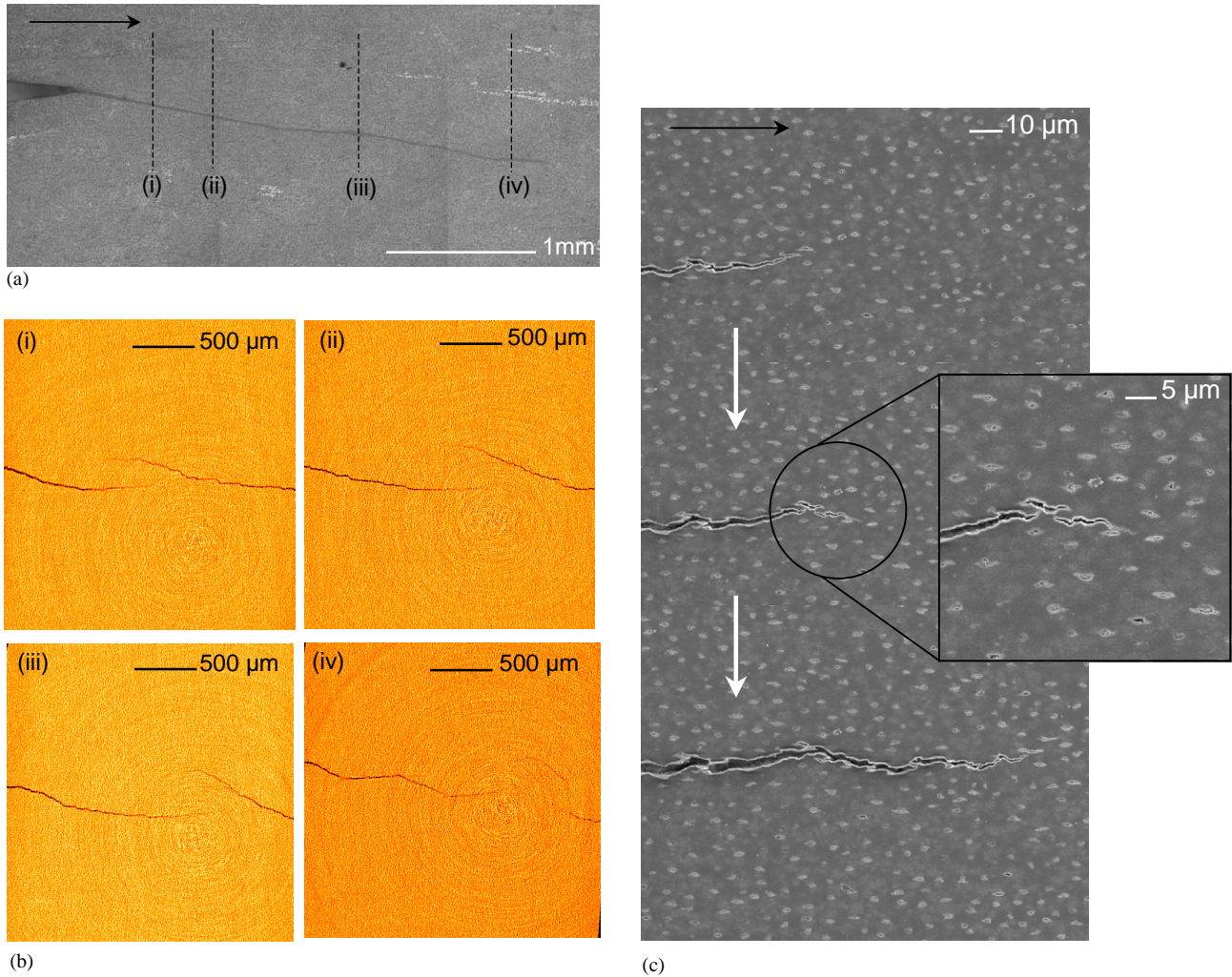


Fig. 4. (a) Optical micrograph showing a typical crack profile in dehydrated dentin. The black arrow indicates the direction of nominal crack growth. (b) Reconstructed computed X-ray tomography slices (at positions shown by the dotted lines in (a)) showing three-dimensional ligament formation in the central portion of the specimen. (c) Scanning electron micrographs illustrating subcritical crack growth in dehydrated dentin tested in vacuo using an in situ loading rig. Very localized uncracked-ligament formation is again apparent; in general the ligaments are considerably smaller in size. Crack extension appears to involve microcracks forming at tubules ahead of the crack which then link up with main crack tip. The black arrow indicates the direction of nominal crack growth; the white arrows show the time-progression of images taken.

compared to the theoretically calculated compliance of traction-free cracks of the same length (using Eqs. (1)–(3)). Results for representative cracks in hydrated and dehydrated dentin are shown in Fig. 6 for two different crack extensions, Δa . It is apparent that the measured compliance is lower than the theoretical compliance for both hydrated and dehydrated dentin, which lends strong support to the notion that the observed bridges indeed sustain a portion of the applied load, thereby providing additional resistance to crack opening. Indeed, if another mechanism was primarily responsible for the R-curve behavior, such as micro-crack toughening, the measured compliance would *not* be higher than the theoretical value. Furthermore, the data suggest that the magnitude of bridging for small crack extensions in dehydrated dentin (Fig. 6b) is significantly smaller than for hydrated dentin (Fig. 6a);

however, these differences are not apparent at longer crack lengths (Figs. 6c and d).

In addition to such qualitative verification of the existence of crack bridging, a quantitative estimate of their contribution to toughening can be obtained from the compliance results. The additional load sustained at the load-line, P_{br} (Fig. 7), can be used to roughly estimate the bridging contribution to the toughness, K_{br} , by assuming P_{br} is applied at the load line and computing K_{br} based on the standard $C(T)$ stress-intensity solution [27]. It is important to note, however, that in reality the measured P_{br} is the result of bridging stresses, σ_{br} , distributed along the crack wake (Fig. 8) and the precise determination of the toughening contribution requires knowledge of the full bridging stress distribution. Accordingly, the estimates for K_{br} described below must be considered as only approxima-

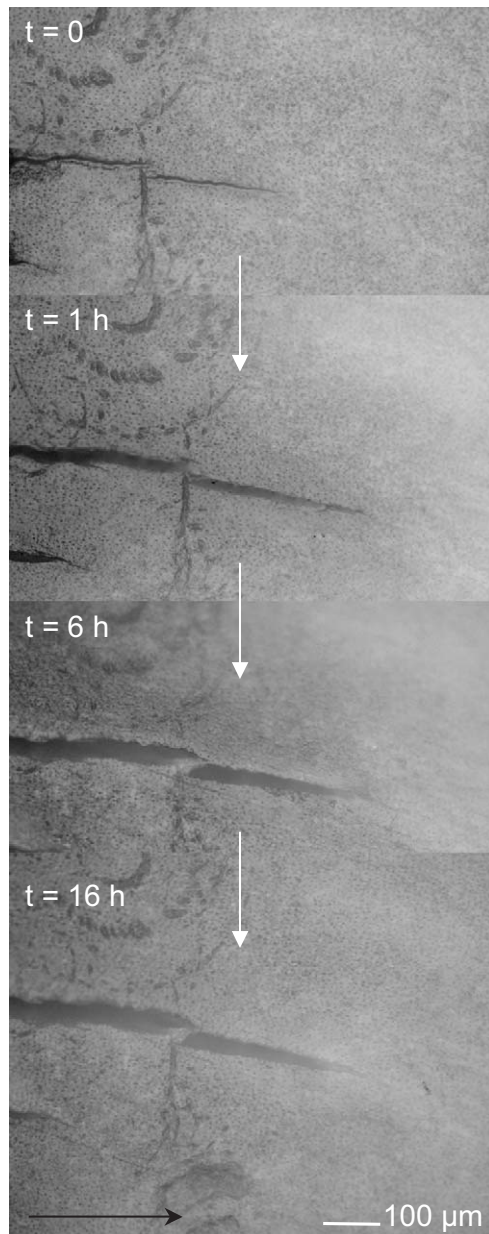


Fig. 5. Optical micrograph (at zero load) illustrating the blunting phenomenon in hydrated dentin. There is some initial crack growth (from $t = 0$ to 1 h), but time-dependent permanent deformation (“blunting”) is clearly apparent. The white arrows indicate the time progression of the series, while the black arrow indicates the direction of nominal crack growth. There is also some evidence of uncracked-ligament bridging.

tions, although they are useful for comparative purposes. For short crack extensions of $\Delta a \sim 1$ mm (Figs. 6a and b), bridging loads of $P_{br} \sim 6.3$ and 0.5 lbs were obtained, respectively, for hydrated and dehydrated dentin. This corresponds to toughening contributions from crack bridging of, respectively, $K_{br} \sim 0.4$ and < 0.1 MPa \sqrt{m} for hydrated and dehydrated dentin, indicating that the bridging contribution was relatively small at short crack extensions in the dehydrated case.

However, for longer crack extensions of $\Delta a \sim 5$ mm (Figs. 6c and d), the calculated bridging contributions for both cases were very similar ($K_{br} \sim 1$ MPa \sqrt{m}). These results provide convincing (qualitative and quantitative) evidence that, despite claims to the contrary [7], a major contribution to toughening in dentin is provided by uncracked-ligament bridging irrespective of hydration.

4. Discussion

The present results confirm that the fracture toughness of dentin displays rising R-curve behavior. Both hydrated and dehydrated dentin show this effect, with both the crack-initiation toughness (K_0) and crack-growth toughness (initial slope of the R-curve) being higher in the hydrated material. One way to understand these trends and to draw a distinction between initiation and growth toughness is to recognize that subcritical crack extension can be considered as the mutual competition between two classes of mechanisms: (i) *intrinsic* toughening mechanisms that operate ahead of the crack tip and act to enhance the material’s inherent resistance to microstructural damage and cracking, and (ii) *extrinsic* toughening mechanisms that operate primarily behind the crack tip by promoting crack-tip shielding, which reduces the local stress intensity actually experienced at the crack tip [17–19]. Intrinsic mechanisms, such as crack blunting, tend to affect the initiation toughness, whereas extrinsic mechanisms, such as crack bridging, promote crack-growth toughness. Since the latter mechanisms operate in the crack wake, their effect is dependent on the size of the crack; this in turn can lead to rising R-curve behavior because after crack extension a more substantial shielding zone can be established in the crack wake.

In the context of this description, the higher crack-initiation toughness of the hydrated dentin can be associated with the evidence of crack blunting, which is promoted by the presence of plasticity and viscoplasticity at the crack tip (Figs. 3 and 5). Indeed, hydration was observed to elevate the initiation toughness by $\sim 60\%$, in terms of K ($K_0 \sim 1.9$ MPa \sqrt{m}), and $\sim 185\%$ in terms of G . Additional evidence for the intrinsic toughening effect of blunting is seen in the dehydrated-rehydrated results (Fig. 2), where an immediate jump in toughness was observed upon hydration before any additional crack extension had occurred. Such blunting serves to lower the stresses experienced ahead of the crack tip. For example, linear-elastic solutions [28] for the stresses ahead of a blunted crack of root radius, ρ , indicate that for any given applied driving force, the tensile stress normal to the crack plane, σ_{yy} , is reduced by 22% and 42% (relative to that of a sharp crack) at distances of, respectively, $\rho/10$ and $\rho/20$ ahead of the

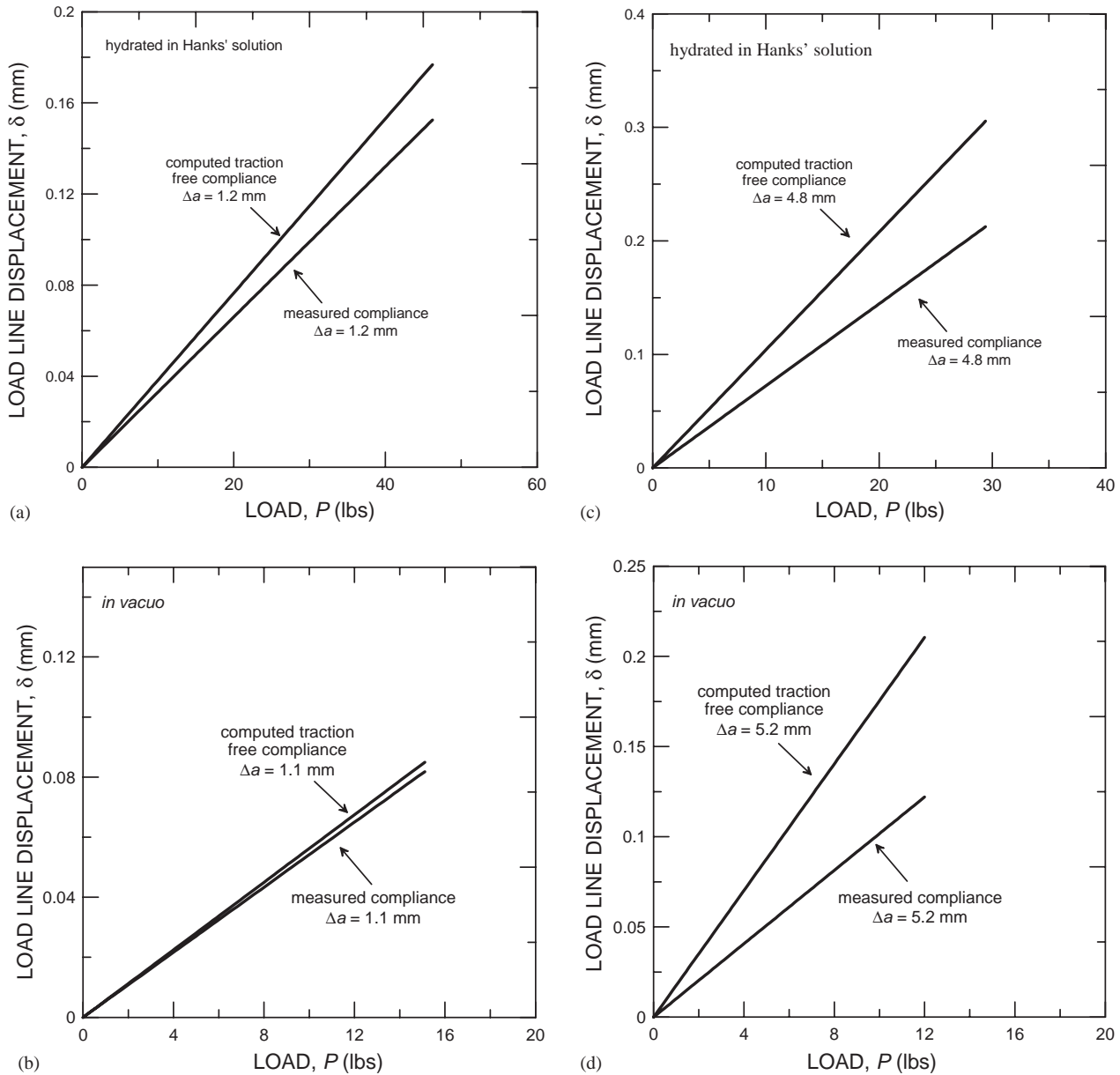


Fig. 6. Computed (traction-free) and measured (bridged) compliance curves, in the form of load-line displacement as a function of applied load, for hydrated (a, c) and dehydrated (b, d) dentin. The observation that the experimentally measured compliance is significantly lower than the compliance of a traction-free crack of the same size is strong evidence for the existence of bridging. For short crack extensions, there was not much bridging in the dehydrated case (b).

tip. While the fracture mechanics aspects of such crack blunting are well characterized, the mechanism for this process in hydrated dentin is yet to be understood, including the fluid egress near the crack tip and time-dependency of the blunting; these remain topics of current study.

The corresponding crack-growth toughness, in the form of rising R-curve behavior, implies the presence of extrinsic toughening mechanisms that develop with crack extension. Additionally, the shape of the R-curve changes quite markedly with hydration, and these differences must be consistent with the identified

toughening mechanisms. While dehydrated dentin showed a flatter, monotonically increasing toughness with crack extension, hydrated dentin showed an initial steep increase in toughness that “flattened out” with further crack extension (Fig. 1b).

In hydrated dentin, uncracked-ligament bridging was by far the most prevalent shielding mechanism observed (Fig. 3). Because bridges can only form with crack extension, this mechanism can only affect the crack-growth toughness; however, eventually a steady-state condition is reached where bridges are formed near the crack tip and destroyed in the crack wake at an equal

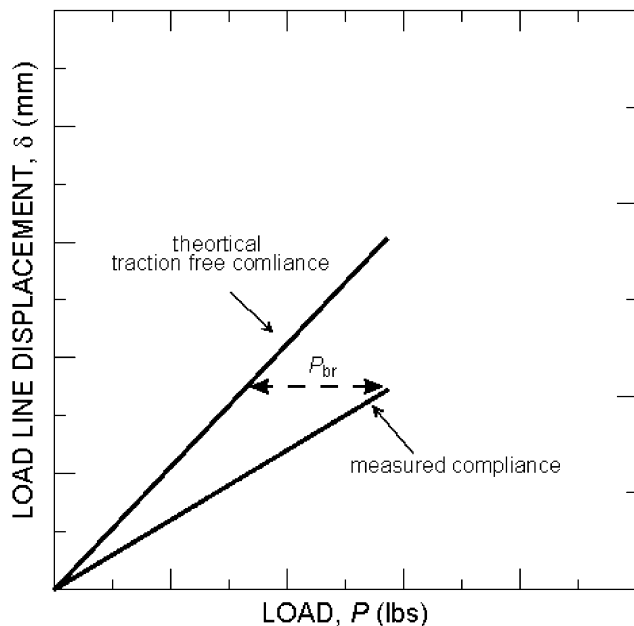


Fig. 7. Schematic showing how the load sustained by active bridges measured at the load line, P_{br} , may be obtained by comparing the measured and theoretical compliance. P_{br} is the additional load which must be applied to the bridged crack to achieve the same load-line displacement as the traction free crack.

rate, leading to the observed plateau in the R-curve. The amount of crack extension to reach this steady state is therefore approximately equivalent in dimension to the size of the bridging zone in the crack wake. The reconstructed tomography images in Fig. 3b clearly show the existence of such bridging ligaments through the thickness of the dentin; the compliance measurements in Figs. 6a and c provide evidence of their effectiveness. Indeed, these reconstructions (Fig. 3b) demonstrate that bridges are being formed with crack extension and destroyed in the crack wake, and that the amount of bridging is decreased farther from the crack tip, i.e., they are consistent with the observed R-curves in hydrated dentin which show a distinct “plateau”. In contrast, bridging in dehydrated samples appears to persist farther behind the crack tip (Fig. 4), consistent with the R-curves being steadily rising (Fig. 1).

Thus, for hydrated dentin, a steady-state toughness is quickly reached, which appears to be a result of the more extensive crack blunting leading to larger crack-opening displacements. For bridged cracks, the extent of the bridging zone behind the crack tip is generally thought to be controlled by a critical crack-opening displacement, u^* (equivalent to the displacement required to fracture a bridge), after which the bridges fail and no longer provide toughening (Fig. 8). Due to the larger crack openings associated with the hydrated condition, it appears that this critical crack-opening displacement is achieved after less crack extension than

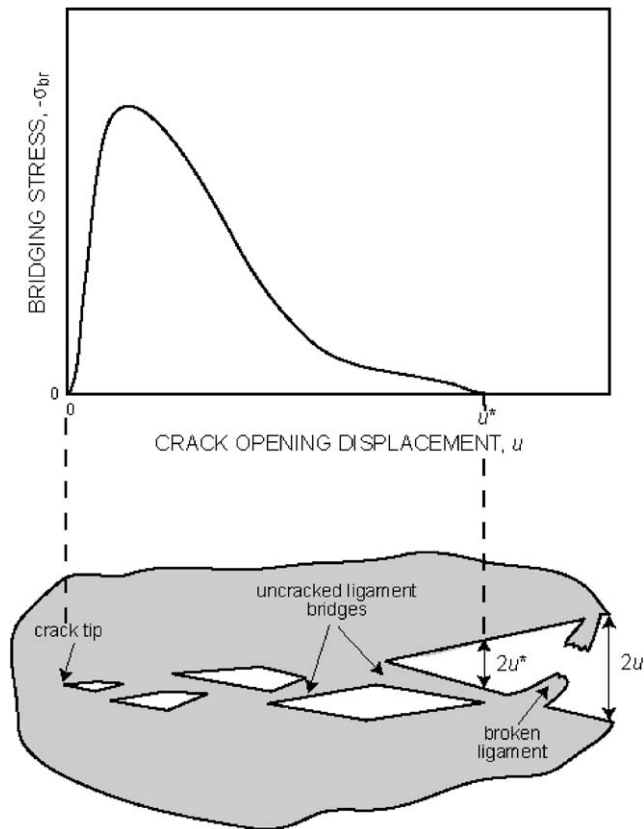


Fig. 8. Schematic illustrating how the bridging stresses, σ_{br} , acting across the crack wake change with position, eventually falling to zero in the region beyond the critical crack opening, u^* . The crack illustrated here represents a steady-state crack, where bridges are being both created at the crack tip and destroyed in the crack wake beyond the critical crack-opening displacement.

in the dehydrated condition. This concept is consistent with the results of the dehydrated-rehydrated experiments where it appears two critical events occur upon rehydration: (i) there is an initial jump in toughness due to crack blunting, and (ii) the blunting causes larger crack openings which in turn lead to the saturation of the bridging zone, so that a steady-state condition is quickly achieved upon rehydration.

In addition to bridging, microcracking has also been suggested as a possible toughening mechanism in hydrated human dentin [7,29]; this mechanism is reasoned to “shield” the crack by creating a dilated zone that surrounds the crack and is constrained by the surrounding (un-microcracked) material. However, in the present study on elephant dentin, the extent of microcracking was minimal, at least in the hydrated material. It is believed that this difference in behavior is associated with the lack of a well-defined, highly mineralized peritubular cuff in elephant dentin, as such cuffs are the prime sites for extensive microcracking in human dentin [29].

While more extensive microcracking was observed to form at tubules ahead of the main crack in dehydrated

dentin, presumably due to the stress concentration there (Fig. 4c), it appears that microcracking in this material is secondary to bridging as a prime toughening mechanism. It is clear though that before linking to the main crack, the presence of these microcracks does provide a mechanism for the formation of uncracked-ligament bridges, although, as noted above, these small near-tip ligaments are believed to only provide minimal toughening. However, the observation of large subsurface ligaments in the crack wake (Fig. 4b) and the compliance results (Fig. 6), clearly indicate that crack bridging can act as a potent toughening mechanism, *even in dehydrated dentin*. These observations contradict previous claims that bridging does not play a substantial role in dehydrated dentin [7]. A comparable role of microcrack toughening in dentin is discounted, as this is not supported by the observed changes in compliance.

In support of the metallographic observations, compliance calculations provide quantitative estimates of the contribution to toughening from the uncracked ligaments. As reported in Section 3.3, such contributions for dehydrated dentin were minimal at short crack extensions ($\Delta a \sim 1$ mm) but were estimated at $K_{br} \sim 1$ MPa \sqrt{m} with further crack growth ($\Delta a \sim 5$ mm); corresponding K_{br} values for hydrated dentin at similar crack extensions were, respectively, 0.4 and 1 MPa \sqrt{m} . Simple theoretical models for uncracked-ligament bridging yield comparable estimates. Using a limiting crack-opening displacement approach [30], K_b values for hydrated and dehydrated dentin can be computed from:

$$K_b = -f_{ul}K_I[(1 + l_{ul}/rb)^{1/2} - 1] / [1 - f_{ul} + f_{ul}(1 + l_{ul}/rb)^{1/2}], \quad (4)$$

where f_{ul} is the area fraction of bridging ligaments on the crack plane (~ 0.85 for hydrated dentin, ~ 0.80 for dehydrated dentin), K_I is the applied (far-field) stress intensity (3.6 MPa \sqrt{m} for hydrated dentin, 2.7 MPa \sqrt{m} for dehydrated dentin), l_{ul} is the bridging-zone size (~ 3.6 mm for hydrated dentin, ~ 2.6 mm for dehydrated dentin), r is a rotational factor (0.195–0.470 [30]) and b is the length of the remaining uncracked region ahead of the crack. Substituting typical values for these parameters, Eq. (4) suggests toughening from crack bridging of the order of $K_b \sim 1.0$ – 1.6 MPa \sqrt{m} for hydrated dentin, and ~ 0.5 – 0.9 MPa \sqrt{m} for dehydrated dentin.

Further understanding of the role of hydration in influencing the fracture resistance of dentin will require a knowledge of how hydration specifically affects its microstructural constituents, particularly the collagen fibrils. Indeed, any factors that modify the mechanical properties of the collagen network would be expected to affect the degree of bridging observed and, conse-

quently, the fracture toughness of dentin. Dehydration has been reported to induce changes in the conformation of partially demineralized human dentin collagen [31] and is known to cause a substantial increase in the stiffness of collagen with a consequent reduction in strength [5,32]. Plasticizing of the collagen fibers and other non-collagenous proteins in dentin on hydration has been suggested to be responsible for such changes [5]. It is also possible that hydration could facilitate sliding between the mineral crystallites occupying the interstices between the collagen fibrils (extrafibrillar mineral); however, it is clear that further investigation in this area is needed.

The relevance of these studies from the perspective of understanding the increased susceptibility of endodontically treated teeth to fracture is debatable since it is unclear if such treatments would result in substantial dehydration of the surrounding dentin [6] or in any significant change in the mechanical properties [33]. If significant dehydration does occur, the present results suggest that the lower initiation toughness and shallower R-curve of dehydrated dentin should lead to easier initiation and propagation of cracks, ultimately causing premature failure as compared to hydrated dentin. However, it should be noted that the dehydrated-rehydrated experiments indicate that rehydration occurs almost immediately, so the dehydrated dentin would need to be completely isolated from liquid for such effects to be significant. What may be a more important factor is that endodontic treatment can introduce flaws which can lead to premature failure of the tooth as a result of catastrophic fracture or, more plausibly, subcritical crack growth induced by cyclic-fatigue loading [34].

Thus in summary, hydration can be seen to significantly increase the fracture toughness of dentin. Mechanistically, this is primarily associated with extensive crack blunting, which elevates the crack-initiation toughness, and additionally from enhanced uncracked-ligament bridging, which promotes the crack-growth toughness and hence results in rising R-curve behavior. In comparison, dehydrated dentin shows little blunting, which results in a lower crack-initiation toughness; however, with crack extension, significant crack bridging occurs, leading to rising R-curve behavior, although the bridging does not develop as quickly as in the hydrated state.

5. Conclusions

Based on a study of the fracture toughness behavior of elephant dentin in hydrated (with Hanks' balanced salt solution) and dehydrated (in vacuo) conditions, the following conclusions can be made:

1. The fracture toughness behavior of dentin can be displayed in terms of rising resistance-curve (R-curve) behavior.
2. The toughness of dentin in the hydrated state is significantly higher than in the dehydrated state. This was manifest as an increase in both the crack-initiation toughness (by ~60%) and (to a lesser degree) the crack-growth toughness, the latter being associated with a steeper initial slope of the R-curve.
3. Mechanistically, hydration was found to promote extensive crack-tip blunting, which was primarily responsible for the enhanced crack-initiation toughness. By dehydrating and then rehydrating a dentin sample, this increase in toughness and the associated crack-tip blunting was found to be essentially instantaneous. However, with time, the crack-tip blunting continued, indicative of some form of viscoplastic deformation behavior in hydrated dentin.
4. Crack-growth toughening, on the other hand, was primarily associated with crack bridging behind the crack tip in both hydrated and dehydrated dentin. The quantitative effect of such bridging was experimentally verified using compliance measurements. Results were inconsistent with significant toughening due to constrained microcracking.
5. The primary mechanism of crack bridging in both hydrated and dehydrated dentin was found to be induced by the formation of uncracked ligaments in the crack wake. Values of the bridging stress intensities, estimated using compliance measurements, were found to be consistent with model predictions.

Acknowledgements

This work was supported by the National Institutes of Health under Grant No. P01DE09859 (for RKN and JHK) and by the Director, Office of Science, Office of Basic Energy Science, Division of Materials Sciences and Engineering, Department of Energy under No. DE-Ac03-76SF00098 (for JJK and ROR). We also acknowledge the support of the Stanford Synchrotron Radiation Laboratory (SSRL), US Department of Energy, supported by Department of Energy contract DE-AC03-76SF00515. The authors wish to thank David Haupt for assistance with the tomography, Prof. S.J. Marshall for her support and Ms. C. Kinzley, Curator, Oakland Zoo, Oakland, CA for supplying the elephant dentin.

References

- [1] Marshall Jr GW, Balooch M, Tench RJ, Kinney JH, Marshall SJ. Atomic force microscopy of acid effects on dentin. *Dent Mater* 1993;9:265–8.
- [2] Kinney JH, Marshall SJ, Marshall GW. The mechanical properties of human dentin: a critical review and re-evaluation of the dental literature. *Crit Rev Oral Biol Med* 2003;14:13–29.
- [3] Jones SJ, Boyde A. Ultrastructure of dentin and dentinogenesis, in *Dentin and dentinogenesis*, vol. 1 (2). Boca Raton, FL: CRC Press; 1984. p. 81–134.
- [4] van der Graaf E, Ten Bosch J. The uptake of water by freeze-dried human dentine sections. *Arch Oral Biol* 1990;35:731–9.
- [5] Kinney JH, Balooch M, Marshall GW, Marshall SJ. A micro-mechanics model of the elastic properties of human dentine. *Arch Oral Biol* 1999;44:813–22.
- [6] Papa J, Cain C, Messer HH. Moisture content of vital vs endodontically treated teeth. *Endod Dent Traumatol* 1994;10:91–3.
- [7] Kahler B, Swain MV, Moule A. Fracture-toughening mechanisms responsible for differences in work of fracture of hydrated and dehydrated dentine. *J Biomech* 2003;36:229–37.
- [8] Sedgley C, Messer H. Are endodontically treated teeth more brittle? *J Endod* 1992;18:332–5.
- [9] Rasmussen ST, Patchin RE, Scott DB, Heuer AH. Fracture properties of human enamel and dentin. *J Dent Res* 1976;55:154–64.
- [10] Rasmussen ST, Patchin RE. Fracture properties of human enamel and dentin in an aqueous environment. *J Dent Res* 1984;63:1362–8.
- [11] el Mowafy OM, Watts DC. Fracture toughness of human dentin. *J Dent Res* 1986;65:677–81.
- [12] Jameson MW, Hood JA, Tidmarsh BG. The effects of dehydration and rehydration on some mechanical properties of human dentine. *J Biomech* 1993;26:1055–65.
- [13] Imbeni V, Nalla RK, Bosi C, Kinney JH, Ritchie RO. In vitro fracture toughness of human dentin. *J Biomed Mater Res* 2003;66A:1–9.
- [14] Nalla RK, Kinney JH, Ritchie RO. Effect of orientation on the in vitro fracture toughness of dentin: the role of toughening mechanisms. *Biomaterials* 2003;24:3955–68.
- [15] Knott JF. *Fundamentals of fracture mechanics*. London, UK: Butterworths; 1976.
- [16] Lawn BR. *Physics of fracture*. *J Am Ceram Soc* 1983;66:83.
- [17] Ritchie RO. Mechanisms of fatigue crack propagation in metals, ceramics and composites: role of crack-tip shielding. *Mater Sci Eng* 1988;103:15–28.
- [18] Ritchie RO. Mechanisms of fatigue-crack propagation in ductile and brittle solids. *Int J Fract* 1999;100:55–83.
- [19] Evans AG. Perspective on the development of high toughness ceramics. *J Am Ceram Soc* 1990;73:187–206.
- [20] Vashishth D, Behiri JC, Bonfield W. Crack growth resistance in cortical bone: concept of microcrack toughening. *J Biomech* 1997;30:763–9.
- [21] Nalla RK, Kinney JH, Ritchie RO. Mechanistic fracture criteria for the failure of human cortical bone. *Nature Mater* 2003;2:164–8.
- [22] Yeni YN, Fyhrie DP. Collagen-bridged microcrack model for cortical bone tensile strength. In: *Proceedings of the 2001 summer bioengineering conference*, vol. 50. New York, NY: ASME; 2001. p. 293–4.
- [23] Arola D, Rouland JA, Zhang D. Fatigue and fracture of bovine dentin. *Exp Mech* 2002;42:380–8.
- [24] Raubenheimer EJ, Dauth J, Dreyer MJ, Smith PD, Turner ML. Structure and composition of ivory of the African elephant (*Loxodonta africana*). *S Afr J Sci* 1990;86:192–3.
- [25] Saxena A, Hudak Jr SJ. Review and extension of compliance information for common crack growth specimens. *Int J Fract* 1978;14:453–68.
- [26] Kinney JH, Nichols MC. X-ray tomographic microscopy (XTM) using synchrotron radiation. *Annu Rev Mater Sci* 1992;22:121–52.

- [27] Ritchie RO, Yu W, Bucci RJ. Fatigue crack propagation in ARALL laminates: measurement of the effect of crack-tip shielding from crack bridging. *Eng Fract Mech* 1989;32:361–77.
- [28] Creager M, Paris PC. Elastic field equations for blunt cracks with reference to stress corrosion cracking. *Int J Fract Mech* 1967;3:247–52.
- [29] Nalla RK, Kinney JH, Ritchie RO. On the fracture of human dentin: Is it stress- or strain-controlled? *J Biomed Mater Res*, in press.
- [30] Shang JK, Ritchie RO. Crack bridging by uncracked ligaments during fatigue-crack growth in SiC-reinforced aluminum-alloy composites. *Metall Trans A* 1989;20A:897–908.
- [31] Habelitz S, Balooch M, Marshall SJ, Balooch G, Marshall Jr GW. In situ atomic force microscopy of partially demineralized human dentin collagen fibrils. *J Struct Biol* 2002;138:221–36.
- [32] Maciel KT, Carvalho RM, Ringle RD, Preston CD, Russell CM, Pashley DH. The effects of acetone, ethanol, HEMA, and air on the stiffness of human decalcified dentin matrix. *J Dent Res* 1996;75:1851–8.
- [33] Huang TJ, Schilder H, Nathanson D. Effects of moisture content and endodontic treatment on some mechanical properties of human dentin. *J Endod* 1992;18:209–15.
- [34] Nalla RK, Imbeni V, Kinney JH, Staninec M, Marshall SJ, Ritchie RO. In vitro fatigue behavior of human dentin with implications for life prediction. *J Biomed Mater Res* 2003;66A:10–20.